

Artificially Modulated Chemical Order in Thin Films: A  
Different Approach to Create Ferro/antiferromagnetic  
Interfaces

G. Mankey – University of Alabama

et al.

Deposited 07/16/2019

Citation of published version:

Saerbeck, T., et al. (2010): Artificially Modulated Chemical Order in Thin Films: A Different Approach to Create Ferro/antiferromagnetic Interfaces. *Physical Review B*, 82(13). DOI: <https://doi.org/10.1103/PhysRevB.82.134409>

## Artificially modulated chemical order in thin films: A different approach to create ferro/antiferromagnetic interfaces

T. Saerbeck,<sup>1,2,\*†</sup> F. Klose,<sup>1,\*‡</sup> D. Lott,<sup>3</sup> G. J. Mankey,<sup>4</sup> Z. Lu,<sup>4</sup> P. R. LeClair,<sup>4</sup> W. Schmidt,<sup>5</sup> A. P. J. Stampfl,<sup>1</sup> S. Danilkin,<sup>1</sup> M. Yethiraj,<sup>1</sup> and A. Schreyer<sup>3</sup>

<sup>1</sup>Australian Nuclear Science and Technology Organisation, Menai, New South Wales 2234, Australia

<sup>2</sup>School of Physics, University of Western Australia, 35 Stirling Highway, Crawley, Western Australia 6009, Australia

<sup>3</sup>GKSS Research Center, Max-Planck-Str. 1, 21502 Geesthacht, Germany

<sup>4</sup>MINT Center, University of Alabama, Tuscaloosa, Alabama 35487, USA

<sup>5</sup>IFF, Outstation JCNS-Institute Laue Langevin (ILL), Forschungszentrum Juelich, 38042 Grenoble, France

(Received 28 April 2010; revised manuscript received 22 June 2010; published 6 October 2010)

We report on a unique magnetic exchange interaction in a thin film of FePt<sub>3</sub>, comprising an artificially created ferromagnetic (FM)/antiferromagnetic (AFM) modulation, but homogeneous chemical composition and epitaxy throughout the film. The chemical order, on the other hand, is modulated resulting in the formation of alternating FM/AFM layers. To determine the existence and form of the magnetic structure within the monostoichiometric thin film, we use a unique combination of polarized neutron reflectometry, x-ray/neutron diffraction, and conventional magnetometry. This artificial stratified AFM/FM FePt<sub>3</sub> exhibits a high magnetic exchange bias thus opening up possibilities to study such magnetic phenomena in a perfectly lattice-matched system.

DOI: [10.1103/PhysRevB.82.134409](https://doi.org/10.1103/PhysRevB.82.134409)

PACS number(s): 75.70.Cn

Artificially modulated structures have formed the mainstay of modern day magnetism as completely novel magnetic properties may be fabricated, many of which are crucial to numerous spin-electronics applications.<sup>1,2</sup> Typical structures are thin-film multilayers, heterostructures, and superlattices of varying elemental composition and/or stoichiometry, whereby the layering leads to a set of unique, and in some cases, tunable properties.<sup>3</sup> In many of those chemically modulated multilayers, however, the desired physics, such as the exchange-bias (EB) effect, may be affected by incommensurate growth, interface roughness and strain. On the other hand, chemical order, that is, the ordered distribution of the constituent atoms in a material of a single chemical composition, affects magnetic phases and magnetic phase transitions without structural variation, which drives the scientific interest in these systems (see, for example, Refs. 4–6). For example, several magnetic alloys, such as Co<sub>x</sub>Pt<sub>1-x</sub>, Fe<sub>x</sub>Rh<sub>1-x</sub>, and Fe<sub>x</sub>Pt<sub>1-x</sub> have already been investigated in view of their magnetocrystalline anisotropy and magnetic phases depending on chemical order.<sup>7–10</sup>

In this paper we present a unique way to create a modulated antiferromagnetic (AFM)/ferromagnetic (FM) structure without changing material composition or lattice structure but rather based solely on a modulated chemical ordering. In thin films of FePt<sub>3</sub> we control the degree of chemical order through temperature modulation during growth, thus creating a single-crystalline FePt<sub>3</sub> film of homogeneous composition throughout consisting of alternating chemically ordered antiferromagnetic and chemically disordered ferromagnetic layers. Since AFM and FM phases of the same material coexist at the same temperature, this multilayer shows a distinctive structural and electronic compatibility at the interface between different layers, i.e., no lattice mismatch, identical chemical composition and similar electronic structure. Therefore it offers the intriguing possibility to study intrinsic magnetic exchange coupling phenomena between two mag-

netic phases of a single crystal. In the progress of this paper we will illustrate the successful preparation and complete characterization of our magnetically modulated quasisingle-crystal FePt<sub>3</sub> thin film. Although structurally very simple, this artificially created material shows a unique self-exchange biasing effect, whose physics is only governed by direct magnetic exchange between different magnetic phases of FePt<sub>3</sub>. A combination of magnetically sensitive neutron techniques is used to verify the modulated AFM/FM nature of the thin-film structure, separating the unique magnetic structure from the compositionally homogeneous thin film.

In general, the crystal structure of FePt<sub>3</sub> is similar to Cu<sub>3</sub>Au which is prototypical for a chemical order-disorder transition.<sup>11</sup> Stoichiometric FePt<sub>3</sub> bulk crystals in perfectly chemically ordered face-centered-cubic (fcc) L1<sub>2</sub> structure show antiferromagnetic order below  $T_N=160$  K.<sup>12</sup> In this structure, the chemical order corresponds to the Fe atoms occupying the corners and Pt atoms located at the faces of the cubic cell. The Fe moments ( $m_{Fe}=3.3 \mu_B$  extrapolated to  $T=0$  K) order on (110) alternating ferromagnetic subsheets while the Pt atoms carry a small moment ( $m_{Pt}<0.2 \mu_B$ ).

Prior to growing films with chemical order modulation, we established the growth conditions of individual FePt<sub>3</sub> films at different substrate temperatures.<sup>13</sup> The films were grown via magnetron sputtering on MgO(001) substrates and compositionally calibrated to better than 1 at. % using Rutherford backscattering spectrometry. Depositing the FePt<sub>3</sub> films at substrate temperatures  $T_S$  in the range of 873 to 973 K resulted in epitaxial growth with a high degree of chemical order. The FePt<sub>3</sub> layers grow along the (001) direction as determined by x-ray diffraction. A  $\phi$  scan of the (220) reflection performed at  $\phi=45^\circ$  showed a fourfold symmetry and confirmed the epitaxial nature of the films with no in-plane rotation between the MgO(001) substrate and the FePt<sub>3</sub>(001) layers. The (001) reflection is structure factor forbidden in a fcc lattice and its presence allows to quantify the degree of

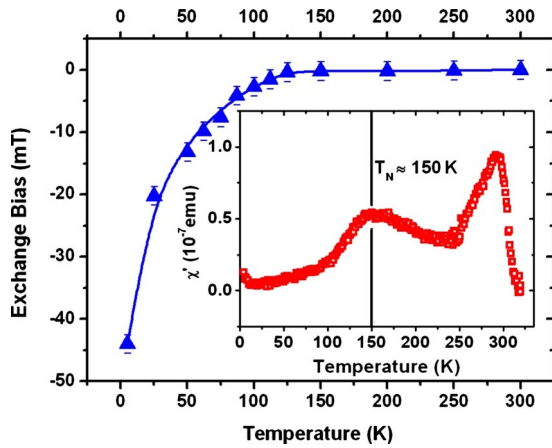


FIG. 1. (Color online) Exchange bias after field cooling to 5 K in an applied field of 1 T (the line is a guide to the eyes). Inset: ac susceptibility as a function of temperature

chemical order in  $\text{Cu}_3\text{Au}$ -type systems (for details, see Ref. 13). By comparing the intensities of the (001) and the (002) reflections the following order parameters were determined:  $S=89\%$  ( $T_S=873$  K) and  $S=99\%$  ( $T_S=973$  K). Thus,  $\text{FePt}_3$  layers grown in this temperature range are highly ordered chemically ( $S=100\%$  corresponds to perfect chemical order). Chemical disorder involving random exchange of Fe and Pt atoms is introduced by lowering the growth temperature. For  $\text{FePt}_3$  films grown at  $T_S=673$  K the (001) reflection was found to be completely absent and the resulting chemical order parameter to be  $S=0\%$ .

Alternating the substrate temperature between  $T_S=937$  K and  $T_S=673$  K during the growth of the films resulted in the highest degree of order modulation but lead to reduced interface qualities due to prolonged cooling procedures. According to x-ray diffraction analysis, a reduced growth temperature of  $T_S=873$  K for the ordered material still results in a very high degree of modulation without compromising interface sharpness as well as reducing impurity adsorption.<sup>13</sup> Therefore, in this study, the magnetic properties of a superlattice of five repetitions  $200 \text{ \AA}$   $\text{FePt}_3$  ( $T_S=873$  K  $\Rightarrow S=89\%$ )/ $100 \text{ \AA}$   $\text{FePt}_3$  ( $T_S=673$  K  $\Rightarrow S=0\%$ ) are presented. As a direct effect of the chemical order modulation, AFM/FM interfaces are created which leads to magnetic exchange bias as determined using vibrating sample magnetometry (VSM). Figure 1 shows the exchange-bias field measured from low to high temperatures after cooling the sample in a 1 T field. With increasing temperature the initial exchange bias of  $H_E=44$  mT at 5 K rapidly decreases until it is no longer detectable at temperatures higher than 150 K. A comparison with experimental exchange bias fields from different systems is difficult since in the literature reported values are widely spread and strongly depending on growth technique, conditions, and interface characteristics (see Refs. 14–17 for recent comprehensive reviews on exchange bias). However, in comparison to the biasing effect in a similarly prepared lattice matched  $\text{CoPt}_3/\text{FePt}_3$  system we investigated earlier, an enhancement of 30% of the exchange field is observed.<sup>18</sup> The widespread of EB values not only gives a motivation for further investigations but impressively high-

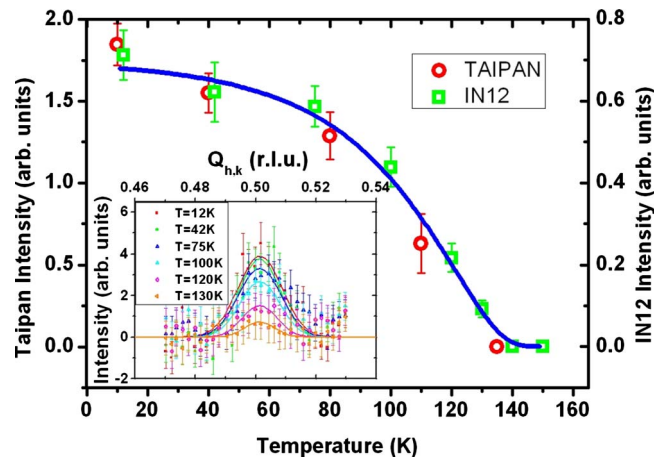


FIG. 2. (Color online) Integrated antiferromagnetic Bragg peak intensities as a function of temperature. The squares represent the data recorded at IN12, which are shown in the inset (symbols = data and lines = Gaussian fits). The circles have been recorded with TAIPAN in similar geometry to IN12 (profiles not shown).

lights the complex manner of the origin of the effect.<sup>14</sup> Since exchange bias is agreed to be an interfacial dominated effect,<sup>19</sup> detailed knowledge of magnetic and structural properties of the interface is crucial for understanding exchange anisotropies between different magnetic phases. Here, due to elimination of structural uncertainties by ensuring homogeneous single-crystalline quality of both phases throughout the interface, the observed exchange bias is arising from pure magnetic exchange interactions, unaffected by structural contributions. As such, this material exhibits the unique opportunity to study purely magnetic exchange interactions, as exchange bias, completely without structural assumptions. The  $H_E$  enhancement with respect to  $\text{CoPt}_3/\text{FePt}_3$  can be understood taking into account the reduced temperature during growth of the chemically ordered structure leading to additional FM/AFM phase separation and interfaces within the layer with an order parameter of  $S=89\%$ . This will be discussed in more detail further below. The inset of Fig. 1 shows the temperature dependence of the ac susceptibility (a 5 Oe/1000 Hz oscillating field was applied in the plane of the sample). The observation of two peaks, corresponding to two magnetic phase transitions, underlines the magnetic quality of the sample. The narrow peak at approximately 300 K indicates a paramagnetic (PM)/ferromagnetic transition and agrees well with the Curie temperature found for disordered  $\text{FePt}_3$  thin films.<sup>13</sup> The observed Curie temperature, which is slightly above 300 K, is slightly lower than that reported for bulk systems.<sup>20</sup> Centered at 150 K, a second much broader peak is observed which, according to neutron-diffraction data (Fig. 2) and polarized neutron reflectometry (PNR) analysis presented below, can be identified as a true paramagnetic/antiferromagnetic transition. In contrast to strongly coupled thin magnetic bilayers of magnetic material, in which only a single transition is observed,<sup>21,22</sup> FM, AFM, and their transitions, can be clearly separated. The existence of a PM phase in the temperature region  $150 < T < 300$  K indicates a more bulklike behavior of the ordered layer, mostly decoupled from the FM disordered layer. The broadening of the second

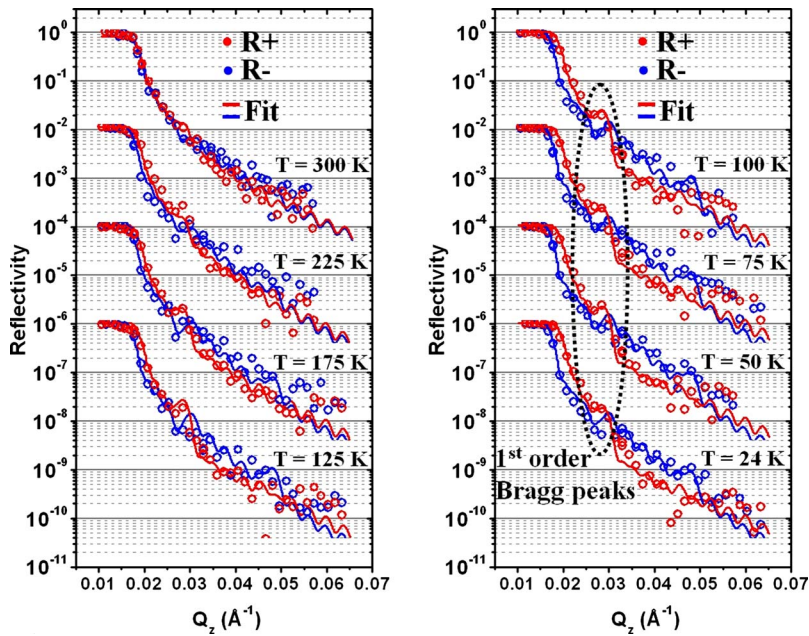


FIG. 3. (Color online) Recorded polarized neutron reflectivity (open symbols) in  $R^+$  (red) and  $R^-$  (blue) polarization and simulations (lines). The data have been background corrected and normalized to 1. Individual data sets have been offset from one another by two orders of magnitude for clarity.

transition peak indicates a wider distribution of AFM ordering temperatures, presumably due to slight local variations in the degree of chemical order. Note that the appearance of the Néel peak at a temperature of 150 K corresponds well to the onset of the observed exchange bias.

In order to further elucidate the antiferromagnetic ordering in the superlattice, high-angle neutron diffraction was performed using the triple-axis spectrometers IN12 (Institute Laue Langevin, Grenoble) and TAIPAN (Australian Nuclear Science and Technology Organisation, Sydney). In both experiments the incoming neutron wavelength was fixed (IN12: 3.141 Å, TAIPAN: 2.35 Å) and the spectrometers were setup to detect elastic scattering. High-angle diffraction peaks of the FePt<sub>3</sub> superlattice were recorded by setting the spectrometer to particular combinations of incident and scattered angles and subsequently measuring rocking curve profiles. Similar to chemically ordered FePt<sub>3</sub> bulk crystals ( $T_N = 160$  K), the superlattice exhibits the onset of a  $(\frac{1}{2} \frac{1}{2} 0)$  AFM Bragg peak below a temperature of 140 K (Fig. 2). Rocking curve profiles recorded at IN12 are shown in the inset of Fig. 2. This half-order magnetic Bragg peak demonstrates the existence of antiferromagnetism within the chemically ordered FePt<sub>3</sub> layers. The main graph in Fig. 2 shows the temperature dependency of the integrated AFM peak intensity. The results from both instruments, TAIPAN and IN12, agree very well with each other. Reference scans measured along the (200) and (220) directions by TAIPAN as well as the (111) and (002) directions measured by IN12 revealed no significant intensity changes with varying temperature, thus indicating ferromagnetic ordering only occurs along these directions. Furthermore, no  $(\frac{1}{2} 0 0)$  reflection could be observed at any temperature, implying the chemically ordered phase of the sample fully orients in the antiferromagnetic  $Q_1$  phase.<sup>12</sup>

A detailed layer-resolved characterization of the magnetic superlattice was carried out using the polarized neutron reflectometer NERO at the GKSS research facility in Geesthacht, Germany. Spin-resolved neutron reflectivity from strati-

fied media is sensitive to depth-dependent chemical and magnetic structures and interfaces making neutrons an excellent tool to study magnetic multilayers.<sup>23</sup> Of particular interest in the current system is the magnetic and nuclear structure and quality of the AFM/FM interface, both can be well separated using PNR. In the experiment the specular reflected intensity of a monochromatized neutron beam ( $\lambda = 4.33 \text{ \AA} \pm 1\%$ ) as a function of incident angle  $\theta$  in different polarization stages ( $R^\pm$ ) is detected. The superscript +(-) denotes the direction of the neutron polarization of the incoming beam as parallel (antiparallel) with respect to the external field direction. Note that the scattering vector is very small in PNR measurements. Therefore, in contrast to high-angle neutron diffraction, PNR is not sensitive to AFM order on atomic scales, but reveals the averaged FM volume magnetization of each layer.

The momentum transfer in the direction parallel to the surface normal ( $z$  direction) is defined by  $Q_z = 4\pi/\lambda \sin \theta$ , where  $\lambda$  is the neutron wavelength and  $\theta$  is the angle of incidence. The data sets in Fig. 3 were recorded from low to high temperatures with an applied field of 620 mT in the plane of the sample in order to saturate the ferromagnetic areas. Prior to the PNR measurements the superlattice was cooled in an external field of 1 T (analogous to the VSM and ac susceptibility measurements) in order to induce an exchange bias. Figure 3 shows reflectivity profiles (open dots) in the temperature range between 24 and 300 K as function of the out-of-plane scattering vector  $Q_z$ . In all measurements only the nonspin-flip channels (i.e., neutron polarization does not reverse upon scattering) produced significant intensities, indicating that the vast majority of the magnetic moments in the sample are aligned with the external field.<sup>24</sup>

Simulations of the experimental PNR data (solid lines in Fig. 3), performed with the polarized neutron reflectivity simulation program SIMULREFLEC,<sup>25</sup> allow the determination of depth-resolved chemical and magnetic structures in form of nuclear and magnetic scattering length density (SLD) profiles (Fig. 4). The structural model consists of a uniform

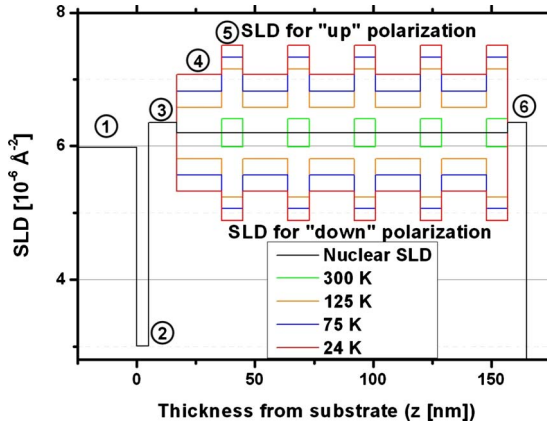


FIG. 4. (Color online) SLD profiles for selected temperatures resulting in the best fit to the PNR data. Different regions in the multilayer are labeled with ① MgO(001) substrate, ② Cr(50 Å) buffer layer, ③ Pt(120 Å) seed layer, ④  $5 \times \text{FePt}_3(200 \text{ Å})$ -ordered, ⑤  $5 \times \text{FePt}_3(100 \text{ Å})$ -disordered, and ⑥ Pt(80 Å) capping layer. SLDs above the nuclear SLD (black line) correspond to parallel polarization while SLDs below correspond to antiparallel polarization with respect to the external magnetic field.

single-crystalline  $\text{FePt}_3$  film of total thickness  $T_t=150 \text{ nm}$  with a calculated scattering length density of  $6.2 \times 10^{-6} \text{ Å}^{-2}$ . Apart from magnetic information, no compositional modulation of the  $\text{FePt}_3$  multilayered structure is included, which can be seen by the flat black line between region ③ and ⑥ in Fig. 4. Only the interfaces of substrate, seed and capping layer have a 0.5–1 nm nuclear root-mean-square (rms) roughness in the simulation. At a temperature of 300 K, close to the Curie temperature of the system, the ferromagnetic magnetization approaches zero and the reflected intensities become almost equal for both neutron polarizations. Therefore the reflectivity at 300 K approaches the reflectivity of a thick single-crystalline film of nonmagnetic  $\text{FePt}_3$ , showing almost no signatures of multilayer modulation. As the superlattice is cooled below the Curie temperature the critical angles of total reflections for opposite neutron polarizations split and provide a measurement of the average volume magnetization of the sample. This magnetization is translated into a magnetic scattering length density and subtracted (added) to the nuclear scattering length density to account for parallel (antiparallel) neutron polarization with respect to the external field (see Fig. 4). As the magnetization increases, a first-order Bragg peak arises at  $Q_z=0.028 \text{ Å}^{-1}$  ( $Q_z=0.030 \text{ Å}^{-1}$ ) in the  $R^+$  ( $R^-$ ) reflectivity. It has to be noted that the contrast at the interface, which determines the height and splitting of the Bragg peaks, is only determined by the magnetic contrast of neighboring layers due to the different averaged volume magnetizations. With decreasing temperature the magnetization of the FM layer steadily increases, whereas a perfect AFM layer should show zero net magnetization at all temperatures. This behavior would lead to continuously increasing contrast between regions ④ and ⑤ of Fig. 4 and subsequently increasing Bragg peak intensities. On the contrary, the first-order Bragg peaks of Fig. 3 (marked region on right-hand side) show an almost constant intensity with temperature, indicating a constant in-

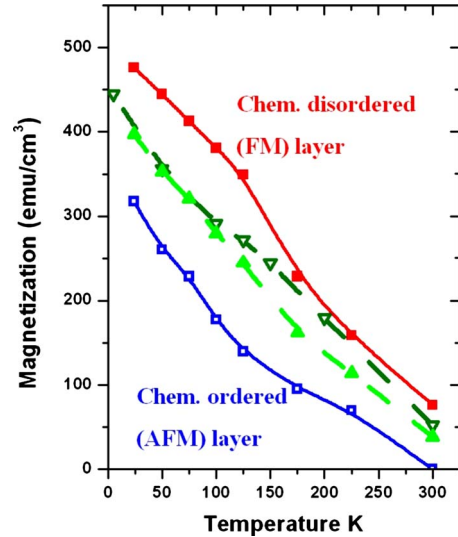


FIG. 5. (Color online) Filled/open squares (red/blue), PNR derived layer-resolved magnetization of the disordered/ordered  $\text{FePt}_3$  layers, respectively. Triangles represent overall volume magnetization as determined by PNR (filled triangles, bright green) and VSM (open triangles, dark green).

terface contrast. Attempting to decrease the interface contrast of higher magnetizations by assuming a magnetic rms roughness of up to 10 nm could not reproduce the experimental results. The best match to the data has been achieved simulating the structure with a magnetic interface roughness of 1 nm (rms) but attributing an essential part of the averaged magnetization to the nominally AFM layers (Fig. 4). Therefore not only FM regions show a split magnetic SLD at lower temperatures but also nominally AFM layers show a similar splitting to the disordered FM layers.

Figure 5 is derived from the simulated profiles in Fig. 4 and shows the layer resolved magnetization as a function of temperature. Tracking the differences in the polarized reflectivities with increasing temperature, the filled/open squares show the evolution of the layer averaged magnetization of the disordered/ordered  $\text{FePt}_3$  layers, respectively. Clearly both layers show a significant increase in magnetization, which adds up to the averaged magnetization of the system (filled green triangles). This behavior suggests the presence of FM domains within the nominal AFM layers. The lateral size distribution of the domains did however not produce any significant off-specular diffuse neutron scattering. Such domains can be understood taking into account the nonperfect growth temperature used to avoid increased magnetic interface roughness and contamination. Figure 5 also shows a comparison of the overall magnetization as analyzed by VSM (filled triangles, green) and PNR (open triangles, dark green). Both VSM and PNR results are in good agreement with each other. The simplicity of our magnetic model, which is sufficient to account for every feature of the real magnetic structure and its behavior in great detail, highlights the successful artificial control of magnetic order and exchange bias within a quasisingle-crystalline film.

To summarize, a magnetic FM/AFM superlattice consisting only of single-crystalline  $\text{FePt}_3$  has been successfully

fabricated by modulation of the chemical order parameter. This artificial phase separation leads to a fascinating material which is exchanged biased with itself in a thoroughly controlled way. Furthermore, the exchange bias is not affected by structural roughness at the interface. The complementarity of x-ray diffraction, polarized neutron, magnetization, and susceptibility measurements allows not only confirmation of the modulated structure but provides a very detailed picture

of the magnetic properties of this unique system. The magnetic superlattice structure reported in this work represents a model system to study magnetic interfaces of exchange-coupled materials with perfect structural interfaces.

G.J.M., Z.L., and P.R.L. gratefully acknowledge financial support from DOE under Award No. DE-FG02-08ER46499.

\*Corresponding author.

†thomas.saerbeck@ansto.gov.au

‡frank.klose@ansto.gov.au

- <sup>1</sup>C. Chappert, A. Fert, and F. N. Van Dau, *Nature Mater.* **6**, 813 (2007).
- <sup>2</sup>S. Parkin, X. Jiang, C. Kaiser, A. Panchula, K. Roche, and M. Samant, *Proc. IEEE* **91**, 661 (2003).
- <sup>3</sup>*Magnetic Heterostructures*, edited by H. Zabel and S. D. Bader (Springer, Berlin, 2008).
- <sup>4</sup>K. R. Coffey, M. A. Parker, and J. K. Howard, *IEEE Trans. Magn.* **31**, 2737 (1995).
- <sup>5</sup>M. E. Gruner, G. Rollmann, P. Entel, and M. Farle, *Phys. Rev. Lett.* **100**, 087203 (2008).
- <sup>6</sup>S. Sun, C. B. Murray, D. Weller, L. Folks, and A. Moser, *Science* **287**, 1989 (2000).
- <sup>7</sup>R. F. C. Farrow, D. Weller, R. F. Marks, M. F. Toney, S. Hom, G. R. M. Harp, and A. Cebollada, *Appl. Phys. Lett.* **69**, 1166 (1996).
- <sup>8</sup>S. S. A. Razee, J. B. Staunton, B. Ginatempo, F. J. Pinski, and E. Bruno, *Phys. Rev. Lett.* **82**, 5369 (1999).
- <sup>9</sup>J. B. Staunton, S. Ostanin, S. S. A. Razee, B. L. Gyorffy, L. Szunyogh, B. Ginatempo, and E. Bruno, *J. Phys.: Condens. Matter* **16**, S5623 (2004).
- <sup>10</sup>G. Rossi, R. Ferrando, and C. Mottet, *Faraday Discuss.* **138**, 193 (2008).
- <sup>11</sup>C. Seok and D. W. Oxtoby, *J. Phys.: Condens. Matter* **10**, 45 (1998).
- <sup>12</sup>S. Maat, O. Hellwig, G. Zeltzer, E. E. Fullerton, G. J. Mankey, M. L. Crow, and J. L. Robertson, *Phys. Rev. B* **63**, 134426 (2001).
- <sup>13</sup>Z. Lu, M. Walock, P. LeClair, G. J. Mankey, P. Mani, D. Lott, F. Klose, H. Ambaye, V. Lauter, M. Wolff, A. Schreyer, H. Christen, and B. Sales, *J. Vac. Sci. Technol. A* **27**, 770 (2009).
- <sup>14</sup>F. Radu and H. Zabel, *Springer Tracts Mod. Phys.* **227**, 97 (2008).
- <sup>15</sup>J. Nogues, J. Sort, V. Langlais, V. Skumryev, S. Suriñach, J. S. Muñoz, and M. D. Baró, *Phys. Rep.* **422**, 65 (2005).
- <sup>16</sup>R. Coehoorn, in *Handbook of Magnetic Materials*, edited by K. H. J. Buschow (Elsevier, Amsterdam, 2003), Vol. 15.
- <sup>17</sup>R. L. Stamps, *J. Phys. D: Appl. Phys.* **33**, R247 (2000).
- <sup>18</sup>D. Lott, F. Klose, H. Ambaye, G. J. Mankey, P. Mani, M. Wolff, A. Schreyer, H. M. Christen, and B. C. Sales, *Phys. Rev. B* **77**, 132404 (2008).
- <sup>19</sup>C. H. Marrows, L. C. Chapon, and S. Langridge, *Mater. Today* **12**, 70 (2009).
- <sup>20</sup>G. E. Bacon and J. Crangle, *Proc. R. Soc. London, Ser. A* **272**, 387 (1963).
- <sup>21</sup>A. Aspelmeier, M. Tischer, M. Farle, M. Russo, K. Baberschke, and D. Arvanitis, *J. Magn. Magn. Mater.* **146**, 256 (1995).
- <sup>22</sup>U. Bovensiepen, F. Wilhelm, P. Srivastava, P. Pouloupoulos, M. Farle, A. Ney, and K. Baberschke, *Phys. Rev. Lett.* **81**, 2368 (1998).
- <sup>23</sup>C. F. Majkrzak, N. F. Berk, and K. V. O'Donovan, in *Neutron Scattering from Magnetic Materials*, edited by T. K. Chatterji (Elsevier Science, Amsterdam, 2005).
- <sup>24</sup>M. R. Fitzsimmons and C. F. Majkrzak, in *Modern Techniques For Characterizing Magnetic Materials*, edited by Y. Zhu (Kluwer Academic, Boston, 2005).
- <sup>25</sup>Program available from <http://www-llb.cea.fr/prism/programs/simulreflec/simulreflec.html>